Available online at www.sciencedirect.com
SCIENCE DIRECT®
Cement & Concrete Composites 28 (2006) 256–266
Cement & Concrete Composites
www.elsevier.com/locate/cemconcomp

Electrochemical and analytical assessment of galvanized steel reinforcement pre-treated with Ce and La salts under alkaline media

M. Sánchez [a,*], M.C. Alonso [a], P. Cecílio [b], M.F. Montemor [b], C. Andrade [a]

[a] *Dep. Corrosion, Instituto Eduardo Torroja, C. Serrano Galvache, n. 4, 28033 Madrid, Spain*
[b] *Instituto Superior Técnico, ICEMS, DEQ, Av. Rovisco Pais, 1049-001 Lisboa, Portugal*

Available online 17 February 2006

Abstract

The present work aims at evaluating the ability of cerium and lanthanum conversion pre-treatments applied on galvanized rebars to hinder the cathodic process of hydrogen release during the early stages of contact between the rebar and the high alkaline environment of the concrete pores solution. The electrochemical behaviour was assessed by polarization resistance, open circuit potential and scanning vibrating electrode technique (SVET). The chemical composition and the morphology of the pre-treated surfaces were evaluated by X-ray photoelectron spectroscopy and scanning electron microscopy. The substrates were immersed in solutions simulating the concrete interstitial electrolyte. The pH was 13.2. For these conditions, the results showed that conversion pre-treatments based on cerium or lanthanum nitrate did not hinder hydrogen evolution, but they changed the corrosion processes occurring on the galvanized rebar during the early stages of immersion.

Keywords: Rare-earth salts; Hydrogen evolution; Pre-treatment galvanized rebars; Alkaline media

1. Introduction

One of the most important causes of premature failure in reinforced concrete structures is reinforcement corrosion. Many times, the structure design following standards and specifications is not enough for long-term durability and the use of additional protective measures becomes necessary. Among the possible anti-corrosion measures, galvanized reinforcements are usually employed to extend the service life of the rebars in concrete structures [1,2]. By one hand, the galvanized coating is a physical barrier that hinders the contact of the aggressive agents with the steel substrate and, by the other hand, zinc acts as a sacrificial anode, protecting the steel against corrosion.

Zinc is an anphoteric metal, stable over a wide range of pH (6–12.5). At pH above 12.5, zinc dissolution and hydrogen evolution takes place [3,4] producing a continuous dissolution of the metal. However, in the concrete interstitial electrolyte the presence of Ca^{2+} induces further passivation of the metal surface. Some researches have identified a pH > 13.2 [4] as the limit for the passivation ability of the galvanized reinforcement. When the pH of the concrete pore solution is above the passivation limit, zinc dissolution accompanied by hydrogen release takes place as soon as the galvanized rebars are embedded in concrete. These reactions lead to aesthetic changes on the concrete surface that shows bubbles and lead to the formation of gaps at the steel/concrete interface during cement setting. These gaps promote a delay in the development of the bonding forces between the reinforcement and concrete. Although these adherence forces increase with time, generally rising the ones reached by steel rebars [5], the aesthetic effects on the concrete cover remain.

* Corresponding author.
E-mail address: mercesanc@ietcc.csic.es (M. Sánchez).

0958-9465/$ - see front matter © 2006 Elsevier Ltd. All rights reserved.
doi:10.1016/j.cemconcomp.2006.01.004

Chromate conversion layers have been a procedure employed to prevent hydrogen gas evolution and to protect the galvanized rebars [6,7]. These pre-treatments lead to the formation of a Cr-rich protective layer that hinders the cathodic reactions. However, due to the toxicity of Cr(VI) ions, these treatments must be avoided. Besides, the new environmental regulations have prompted research and developed environmentally friendly pre-treatments for the protection of the galvanized steel rebars [8–12]. Furthermore, the actual commercialized Portland cements have limited the content of Cr(VI) in their composition. Among the possible alternatives to the use of chromates, rare-earth salts, are a promising choice because they present good corrosion inhibition properties in addition to environmental friendliness. These pre-treatment layers have proved to confer corrosion protection of galvanized steel substrates exposed to neutral sodium chloride solutions [8,9].

Cerium nitrate has been successfully tested for corrosion protection of galvanized steel substrates either as aqueous corrosion inhibitor, as conversion coating [8,9,13–16] or as dopant for thin organic coatings and hybrid sol–gel coatings [17–19]. The corrosion inhibition properties of cerium have been explained by a cathodic mechanism due to the precipitation of cerium oxide/hydroxide films on the cathodic places [20–23]. Lanthanum ions have been used as aqueous corrosion inhibitor for corrosion protection of aluminium, magnesium and steel [24–26]. Corrosion protection of galvanized steel substrates in the presence of La ions has been attributed to the formation of a film composed of La_2O_3 and $La(OH)_3$ and small quantities of $Zn(OH)_2$ and ZnO [20].

For application on galvanized steel rebars the conversion pre-treatments must be stable under alkaline environment, they reduce corrosion activity during the initial stages of contact of the rebars with the alkaline environment, hindering the hydrogen evolution process during the formation of the protective layers on the surface of the galvanized rebars.

In the present work, the stability of cerium and lanthanum conversion layers as well as their ability to hinder the cathodic process was assessed. Synthetic media simulating the aqueous solution existing in the concrete pores was employed, and short-term tests have been considered because these treatments must be effective since the first instants of contact between the rebar and the alkaline solution. These tests, in simulated concrete pore solutions are necessary to understand the protection ability of the pre-treatments, prior its use on galvanized rebars embedded in concrete.

2. Materials and methods

2.1. Preparation of the substrates and solutions

Corrugated galvanized reinforcements with 6 mm of nominal diameter have been employed to study the stability of Ce and La conversion layers. The galvanized coating was obtained by a commercial hot dip process, with the immersion of the rebar in the zinc bath at 450 °C for 90 s.

Before the formation of the conversion layer the rebar was degreased with acetone and washed with distilled water. Then, the rebars were immersed in the rare-earth salt solution (0.05 M ($Ce(NO_3)_3$) or $La(NO_3)_3$) during 5 min. Finally, the samples were oven-dried at 120 °C for 15 min.

The pre-treated and the non-pre-treated galvanized rebars were immersed in alkaline solutions simulating the concrete interstitial electrolyte at ambient temperature. A saturated calcium hydroxide solution with and addition of 0.2 M of potassium hydroxide has been used to simulate the aqueous alkaline content of the concrete pores, with an approximate final pH of 13.2. This medium has been chosen being more representative of concrete pores solution than calcium hydroxide alone (pH 12.6). And also, because at pH 12.6 the galvanized passivation process is quicker and many times there is not a relevant process with hydrogen evolution.

2.2. Techniques

Different electrochemical techniques were used to evaluate the corrosion behaviour of the pre-treated galvanized rebars: corrosion potential monitoring (E_{corr}), polarization resistance measurements (R_p) and scanning vibrating electrode technique (SVET). The E_{corr} and R_p measurements were carried out in situ using the electrochemical cells described elsewhere [26] with a 551 AMEL potentiostat coupled with a 567 AMEL function generator. Two galvanized rebars and a carbon rod acting as counter electrode were immersed in the alkaline solution ($Ca(OH)_2$ sat + 0.2 M KOH, pH ≈ 13.2). The exposed area was 5.65 cm^2. A saturated calomel electrode was employed as reference electrode. The instantaneous corrosion rate was obtained from the R_p measurements according with Stern–Geary equation [27].

The SVET measurements were performed using an applicable electronics apparatus. The scanned area was 4 mm^2. For SVET tests, rebars were immersed into a similar solution along 24 h. SVET measurements were carried out in situ at periodic times.

The chemical composition of the pre-treated rebar surface was assessed by X-ray photoelectron spectroscopy (XPS). XPS measurements were carried out using a 310 F Microlab (VG Scientific). The spectra were taken in CAE mode (30 eV), using a Mg non-monochromatic anode. The spot of the X-ray beam was around 9 mm^2.

The morphology of the surface was studied by scanning electron microscopy (SEM).

SEM tests were carried out ex situ after various ages of immersion in the alkaline media in a JEOL JMS 5400 microscope equipped with a LINK-ISIS energy dispersive (EDX) for analysing the rare-earth conversion layers composition.

3. Results

3.1. Electrochemical behaviour

Evolution of the E_{corr} and i_{corr} of the rebars (pre-treated and non-pre-treated) are depicted in Fig. 1.

After few hours immersion in the alkaline media (pH 13.2) the potential values of both pre-treated and non-pre-treated rebars were around $-1.35\ V_{SCE}$ (Fig. 1a). At this potential, a cathodic process with hydrogen evolution occurs. After 6 days of immersion, the potential of the reference sample rose to values above $-1\ V_{SCE}$, indicating the cease of the hydrogen evolution. However, the potential of pre-treated rebars, either with Ce or La, rose to more anodic values about one day after.

The corrosion rate measurements (Fig. 1b) are in good agreement with the corrosion potential evolution. During the early stages of immersion, the i_{corr} values were independent of the pre-treatment. A decrease of the corrosion rate was observed earlier for the reference sample. However, after 7 days of immersion, the current density of the non-pre-treated sample stabilized around 10 $\mu A/cm^2$ while the current density of pre-treated rebars decreased to lower values. The i_{corr} decrease should be related with the formation of calcium hydroxizincate crystals which progressively covered the zinc surface. Nevertheless, the high current density values registered after one week indicate that the surface did not fully reach passivation.

SVET results obtained during immersion in the pH 13.2 solution showed that the electrochemical response was

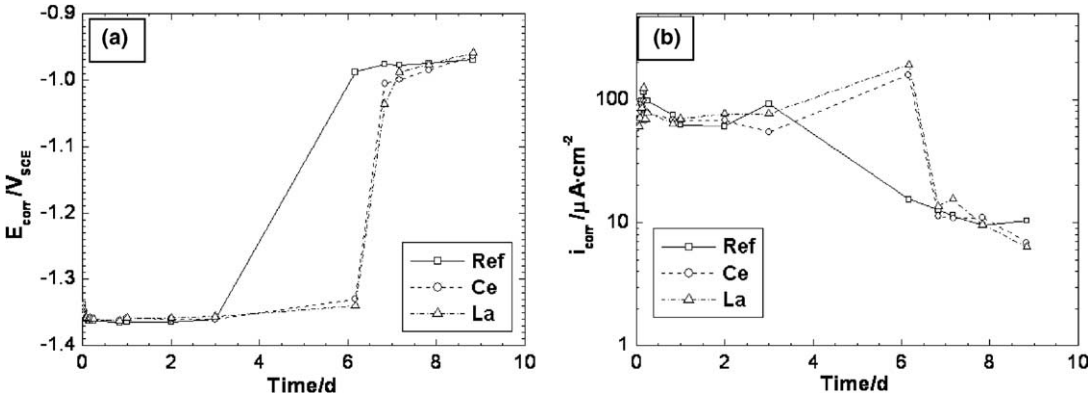

Fig. 1. Electrochemical measurements for rebars immersed in $Ca(OH)_2$ sat + 0.2 M KOH. (a) E_{corr} evolution and (b) i_{corr} evolution.

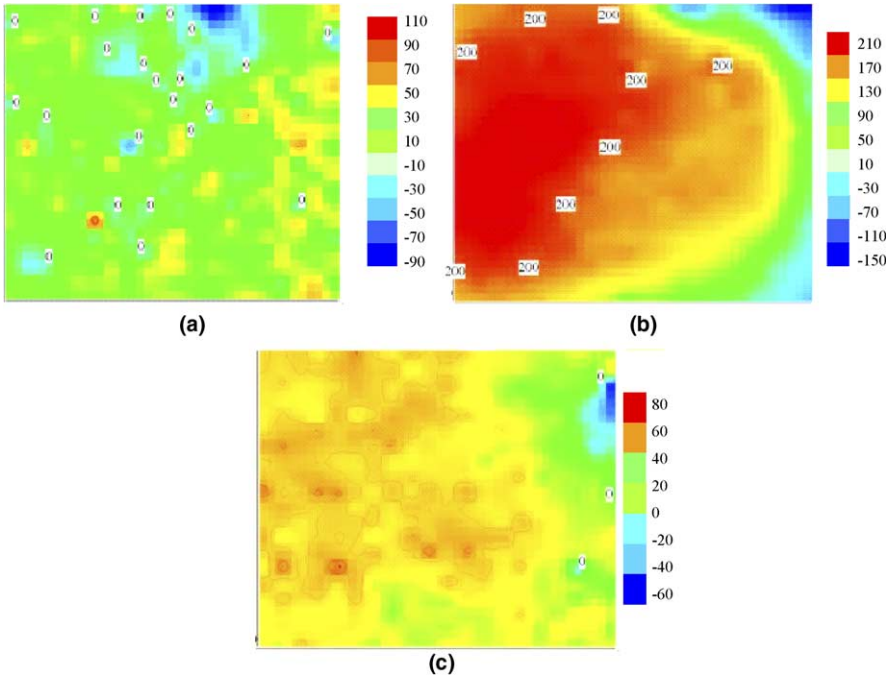

Fig. 2. SVET maps for the reference sample. (a) After few minutes of immersion, (b) after three hours of immersion and (c) after one day of immersion. Units are $\mu A/mm^2$.

dependent on the rebar pre-treatment, as can be observed in Figs. 2–4.

Fig. 2 shows that the anodic activity was randomly distributed over the surface of the non-treated galvanized rebar after few minutes of immersion in the alkaline solution. The surface activity increased during the first 3 h of immersion, but after approximately 1 day the current seemed to decrease due to the growth of the protective layer of corrosion products.

Fig. 3 shows lower activity on the Ce-treated rebar during the initial stages of contact with the alkaline medium comparing with the non-treated rebar. After approximately

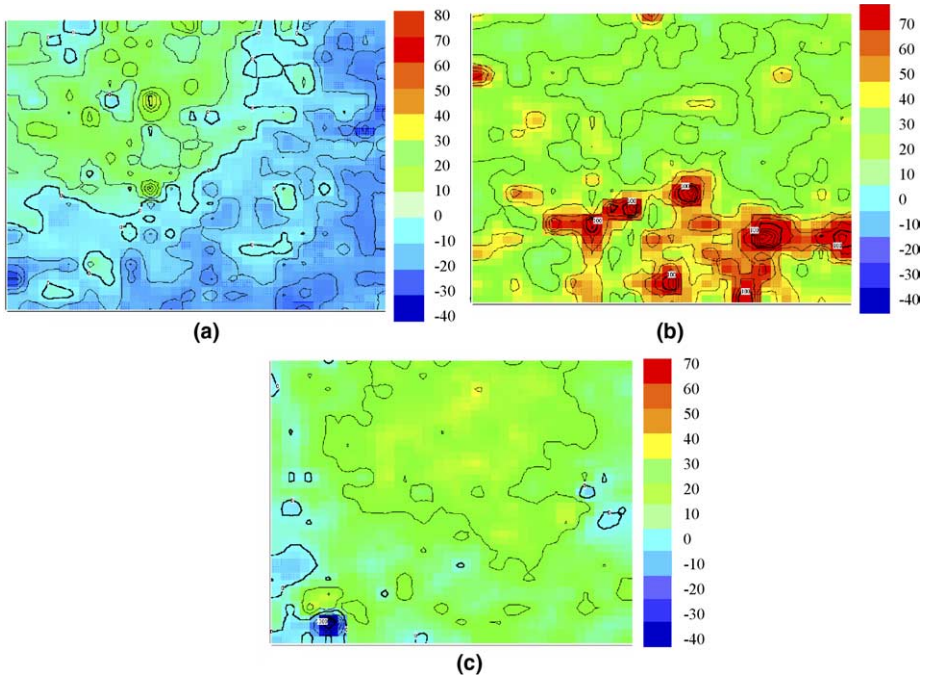

Fig. 3. SVET maps for the Ce-treated sample. (a) After few minutes of immersion, (b) after 4 h of immersion and (c) after one day of immersion. Units are $\mu A/mm^2$.

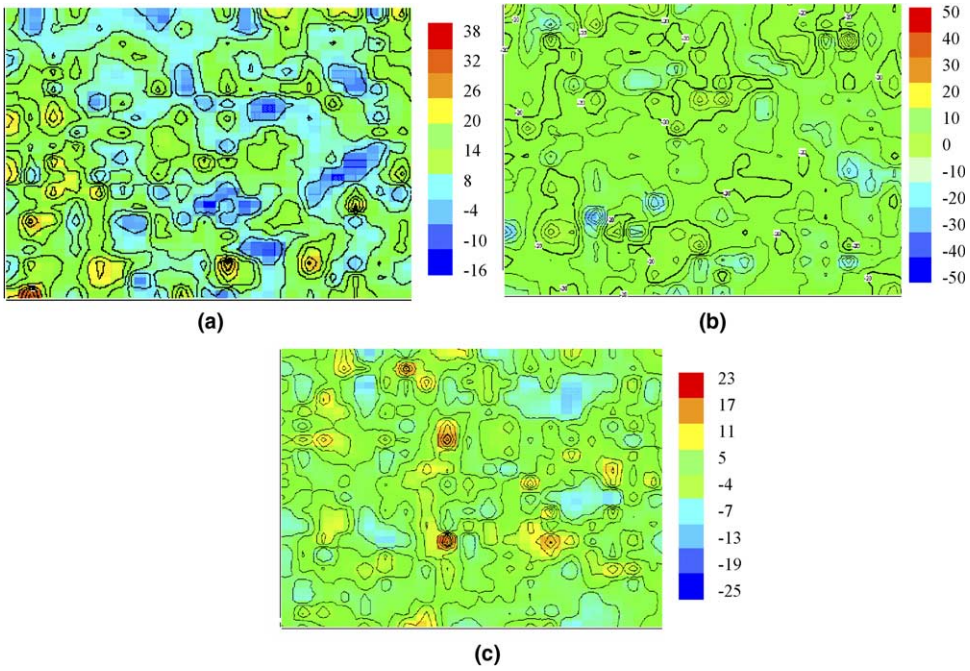

Fig. 4. SVET maps for the La-treated rebar. (a) After few minutes of immersion, (b) after 4 h of immersion and (c) after one day of immersion. Units are $\mu A/mm^2$.

4 h of immersion some anodic activity could be observed on the surface of Ce-treated galvanized rebars. However, latter on, the activity vanished and the anodic currents were reduced.

The evolution of the SVET maps for the lanthanum pre-treated sample was significantly different from that of the reference sample. During the first hours of immersion the surface activity was less intense, no evident anodic spots could be observed over the surface (Fig. 4). However, after about 1 day of immersion signs of increasing activity were measured, being probably associated with the formation of the first nucleus of corrosion products.

It is interesting to note the difference between the R_p and SVET response. The total redox processes occurring on the rebar surface contribute to R_p values. Thus, both anodic and cathodic reactions are measured with the R_p technique. Furthermore, in the Ce-treated rebar, the cerium redox processes are registered by the R_p values. However, it is not possible to quantify the contribution of each process separately by R_p measurements. The application of local techniques, as SVET, revealed interesting features such as the spatial distribution of cathodic and anodic areas over the surface and their variation in time. For the reference rebar, SVET revealed a more generalized corrosion process than for the treated rebars, where a more localized character of corrosion was evidenced. A delay on the development of larger anodic areas for the pre-treated rebars was also observed.

3.2. Analytical characterization

The chemical composition of the rebars was evaluated by XPS. Fig. 5 depicts the XPS spectra for the non-treated galvanized rebar. The amount of zinc hydroxide increased during immersion in the alkaline solution simulating the concrete pores.

In the case of Ce-treated substrates the XPS spectra depicted in Fig. 6 showed that the conversion film was composed by a mixture of Ce(III) and Ce(IV) compounds, probably Ce_2O_3 and/or $Ce(OH)_3$ and CeO_2. The formation of CeO_2 was clearly observed in the O1s spectrum, which evidenced a low energy shoulder around 529.8 eV. After

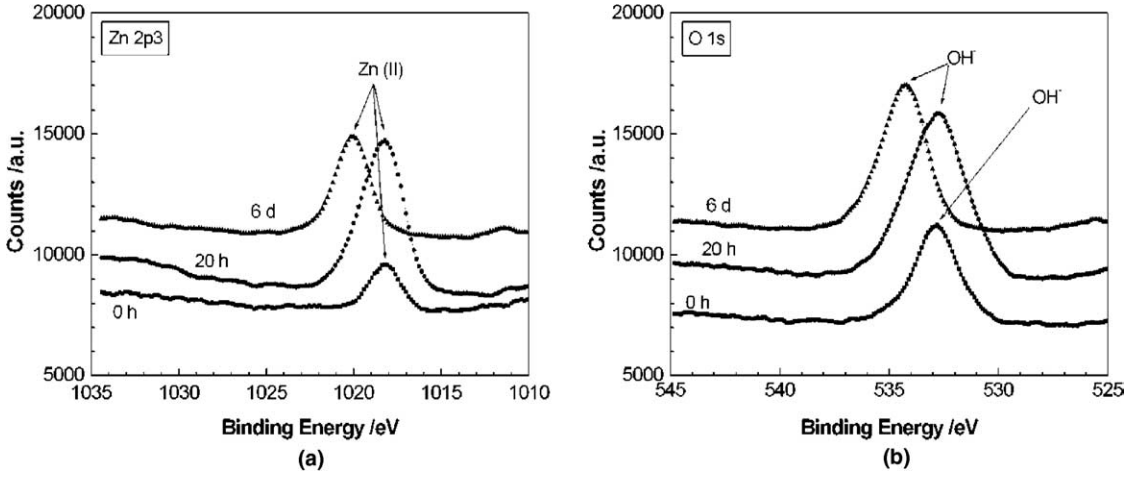

Fig. 5. XPS spectra for the non-treated galvanized rebar. (a) Zn 2p3 and (b) O 1s.

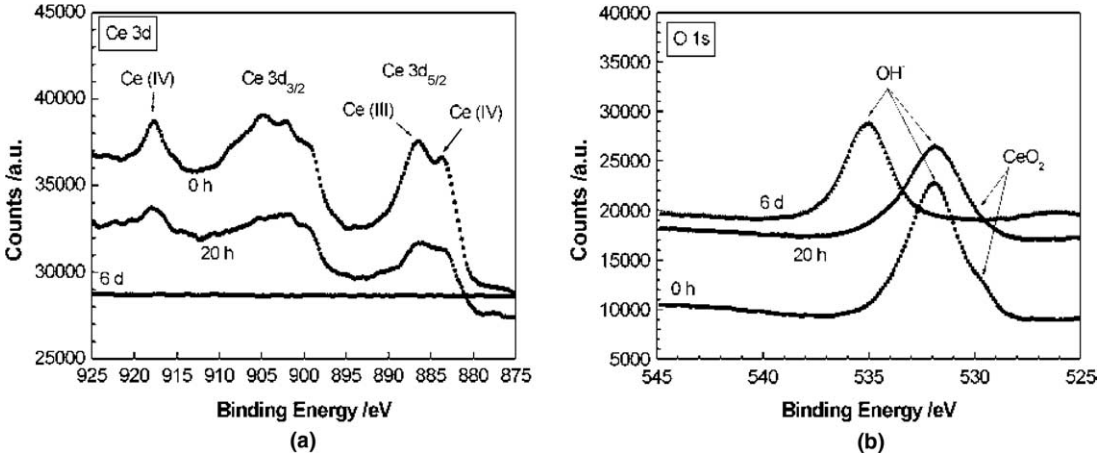

Fig. 6. XPS spectra for the Ce-treated galvanized rebar. (a) Ce 3d and (b) O 1s.

6 days of immersion intensity of the zinc peak increased and cerium could not be detected, showing that all the surface was covered with zinc corrosion products.

The La-treated surface seemed to be composed predominantly by $La(OH)_3$. The composition remains unchanged as the immersion time elapsed. However, the amount of La decreased and, after 6 days of immersion the La signal could not be detected in the XPS analysis – Fig. 7.

The morphology of the surface of the rebars was assessed by SEM. SEM analysis confirmed that the reference sample surface was covered by corrosion products that are likely to be in the form of calcium hydroxizincate, $Ca(Zn(OH)_3)_2 \cdot 2H_2O$ (CaHZn) crystals [28,29], with dimensions that attain a few tens of micrometers (Fig. 8a). In some places these crystals were still growing (Fig. 8b) after 6 days of immersion.

The morphology of the Ce-treated surface was significantly different. After 1 day of immersion the images showed the presence of Ce-oxide grains on the surface (Fig. 9a). The images also revealed the presence of zones where zinc was corroding. After 6 days of immersion no signs of the Ce film could be observed and the surface seemed to be uniformly covered with corrosion products (Fig. 9b) in agreement with the XPS results.

Fig. 10 shows the EDX composition of Ce grains after one day of immersion in the alkaline medium. It could be observed a rich Ce concentration over the precipitated grains.

After approximately one day of immersion the SEM images obtained on the La-treated rebar revealed the presence of some areas covered with zinc corrosion products. Nevertheless, in some places was still possible to observe the presence of the La conversion film (Fig. 11a), which was not continuous, showing several microcracks. After 6 days of immersion the amount of corrosion products increased and several isolated crystals of CaHZn appeared on the surface. Residual La film was still observed after 6 days of immersion on the surface of this rebar, revealing that the growth of the corrosion products layer was delayed by the presence of the conversion film (Fig. 11b).

In Figs. 12 and 13 the EDX composition of La conversion layer after 1 day and 6 days of immersion in the

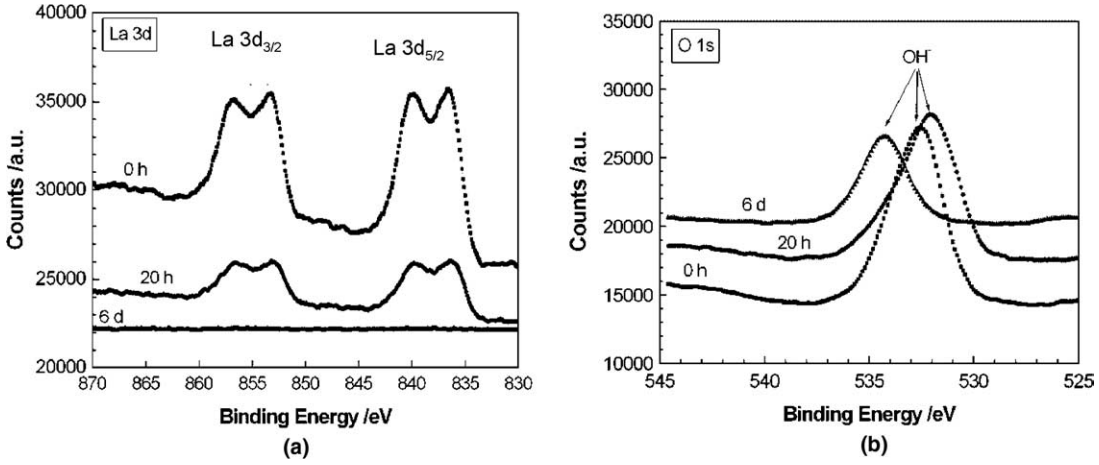

Fig. 7. XPS spectra for the La-treated galvanized rebar. (a) La 3d and (b) O 1s.

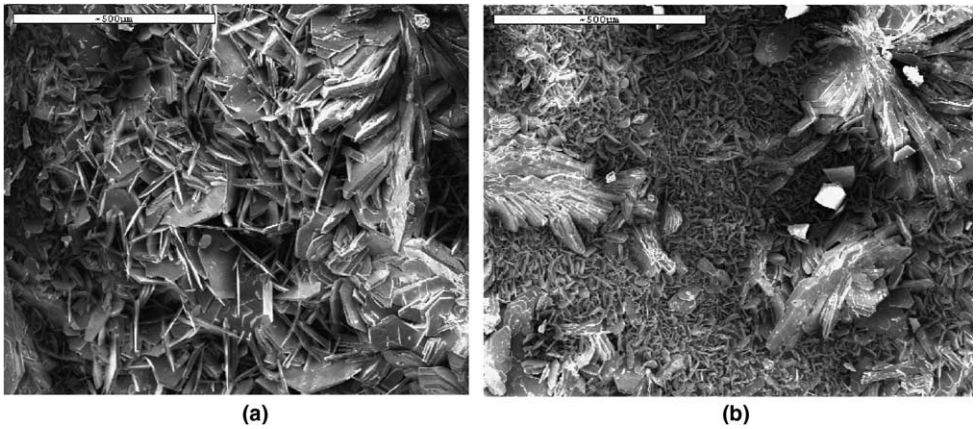

Fig. 8. SEM pictures obtained for the reference sample after 6 days of immersion in alkaline media. (a) Calcium hydroxyzincate crystals growth and (b) calcium hydroxyzincate crystals still growing.

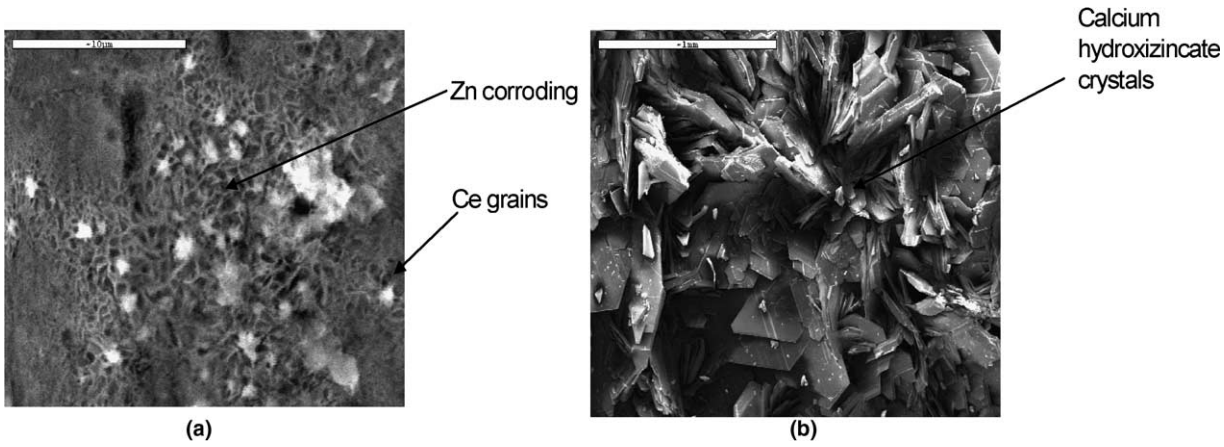

Fig. 9. Ce-treated sample SEM images: (a) 1 day immersion and (b) 6 days immersion.

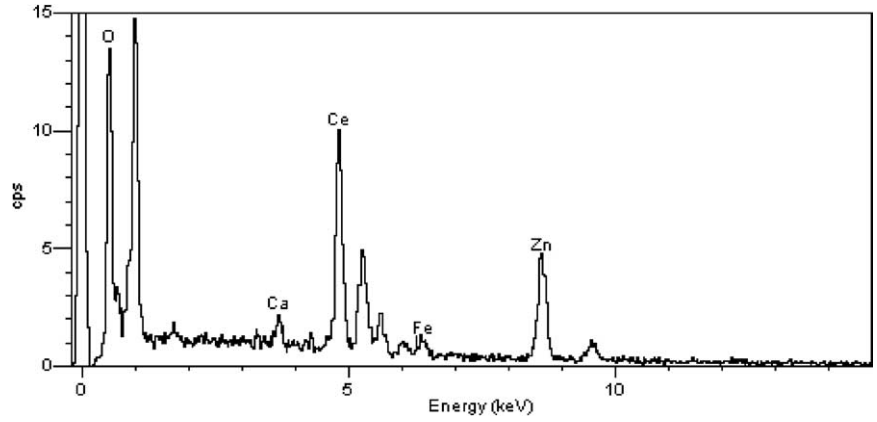

Fig. 10. EDX composition of Ce grains after one day of immersion in the alkaline medium.

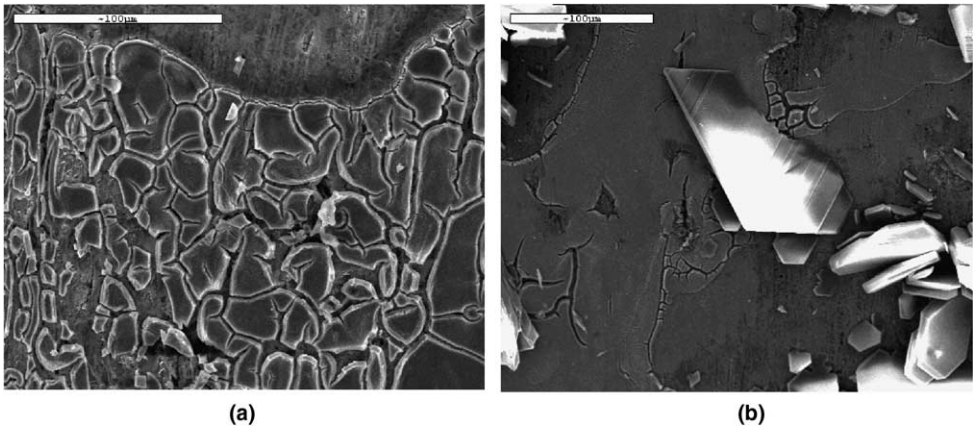

Fig. 11. SEM of La-treated sample: (a) 1 day of immersion and (b) 6 days of immersion.

alkaline medium, respectively, is shown. A decrease in the ration La/Zn concentration ratio was observed.

4. Discussion

In the present work different electrochemical techniques, providing different types of information, were applied to gain knowledge on the behaviour of cerium or lanthanum conversion layers formed on galvanized rebars in solutions simulating the high alkaline environments of the concrete pores solution. In this work the open circuit potential measurements and the polarization resistance (R_p) results clearly showed that the pre-treatments were not able to hinder hydrogen evolution process. However, the results

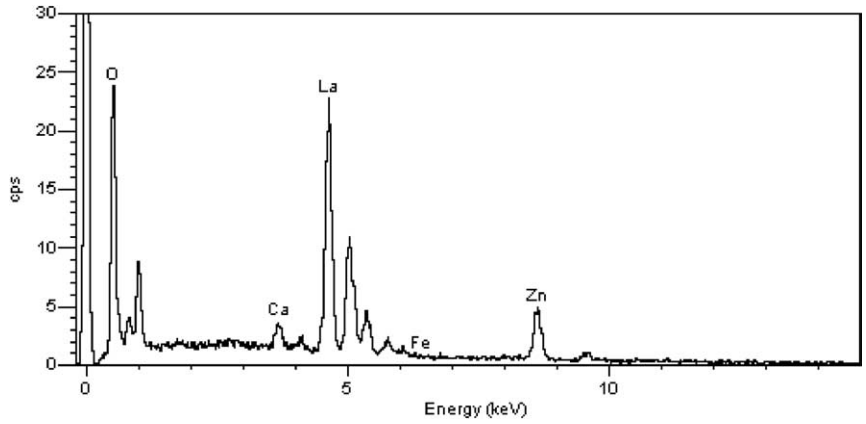

Fig. 12. EDX composition of La conversion layer after 1 day of immersion in the alkaline solution.

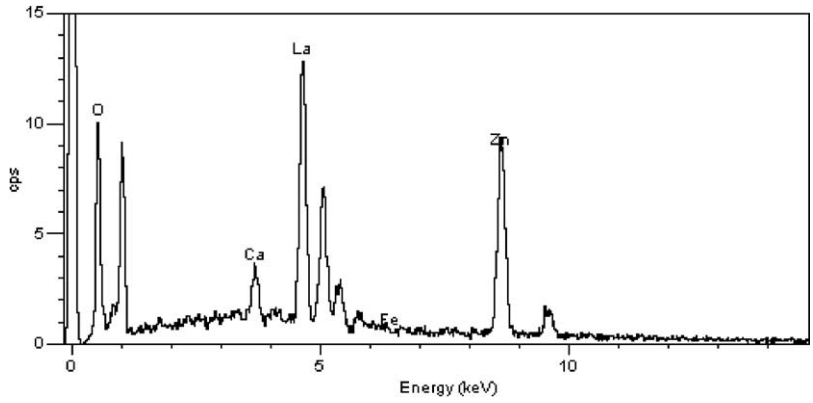

Fig. 13. EDX composition of La conversion layer after 6 days of immersion in the alkaline solution.

showed that are some interesting differences concerning the presence and type of pre-treated galvanized layers. The corrosion processes in the pre-treated rebars seem to be supported by microanodes and microcathodes, while the non-treated samples revealed a more generalized dissolution corrosion process since the early stages of immersion.

The immersion of the galvanized rebars in alkaline solutions promotes the formation of a zinc hydroxide film, although for pH > 12.9 the main anodic product is the soluble zincate ion (ZnO^{2-}) [30]. However, in presence of Ca^{2+} ions, the precipitation of calcium hydroxyzincate crystals, CaHZn takes place over the rebar surface, leading to passivation of zinc [31]. Liebau [32] proposed the following mechanism to explain the formation of CaHZn ($Ca(Zn(OH)_3)_2$) crystals:

$$Zn + 2H_2O \leftrightarrow Zn(OH)_2 + H_2 \quad (1)$$

$$2Zn(OH)_2 + 2H_2O + Ca(OH)_2 \rightarrow Ca(Zn(OH)_3)_2 \cdot 2H_2O \quad (2)$$

4.1. Ce pre-treated rebars

When the galvanized rebars are pre-treated in the cerium nitrate solution anodic dissolution of zinc (Eq. (3)) and cathodic reduction of molecular oxygen take place (Eqs. (4) and (5)) [34]:

$$Zn \rightarrow Zn^{2+} + 2e^- \quad (3)$$

$$O_2 + H_2O + 2e^- \rightarrow H_2O_2 + 2OH^- \quad (4)$$

$$H_2O_2 + 2e^- \rightarrow 2OH^- \quad (5)$$

Then a passive film of zinc hydroxide precipitates over the rebar surface (Eq. (6)) which gradually changes to zinc oxide (Eq. (7)):

$$Zn^{2+} + 2OH^- \rightarrow Zn(OH)_2 \quad (6)$$

$$Zn(OH)_2 \rightarrow ZnO + H_2O \quad (7)$$

The presence of Ce^{3+} ions in the solution promote the formation of a conversion layer of $Ce(OH)_3$ on the zinc surface (Eq. (8)) that changes to oxide (Eq. (9)) [34], forming a thick film composed of $Ce(OH)_3$ (outer layer) and Ce_2O_3 (inner layer):

$$Ce^{3+} + 3OH^- \rightarrow Ce(OH)_3 \quad (8)$$

$$2Ce(OH)_3 \rightarrow Ce_2O_3 \quad (9)$$

According to literature [12] the growth of the Ce(III)-rich oxide and hydroxide layers can take place by direct reaction between Zn(II) and Ce(III) compounds (Eqs. (10)–(13)), constructing a framework of Ce(III) oxide layer containing H^+:

$$[Zn]OH + Ce(III)OH_2 \rightarrow [Zn]OCe(III)OH_2 + H^+ \quad (10)$$

$$[Zn]OH + Ce(III)OH^- \rightarrow [Zn]OCe(III)OH^- + H^+ \quad (11)$$

$$[Zn]OCe(III)OH_2 + Ce(III)OH_2 \rightarrow [Zn]OCe(III)OHCe(III)OH_2 + H^+ \quad (12)$$

$$[Zn]OCe(III)OH^- + Ce(III)OH^- \rightarrow [Zn]OCe(III)OCe(III)OH^- + H^+ \quad (13)$$

The presence of H_2O_2, resulting from oxygen reduction, promotes the formation of Ce^{4+} due to oxidation of Ce^{3+} (Eq. (14)) [33,34]:

$$2Ce^{3+} + H_2O_2 \rightarrow 2Ce^{4+} + 2OH^- \quad (14)$$

Thus, the Ce conversion layer is composed by Ce(III) and Ce(IV) compound as has been confirmed with XPS results for the Ce-treated galvanized rebar before the immersion in the alkaline solution.

When the Ce-treated galvanized rebars are immersed in the alkaline media, the presence of the cerium conversion layer delays the onset of corrosion activity. This behaviour could be demonstrated by the SVET measurements, where no anodic areas could be observed during the first instants of immersion. However, latter on more important activity could be observed, suggesting that the protection provided by the cerium layer was destroyed.

The results suggest that an oxidation of Ce(III) compounds may take place. This agrees with the increase of the ratio Ce(IV)/Ce(III) obtained by XPS data (Table 1).

This increase can be related, according with Pourbaix diagram [35] (Fig. 14), with the formation of hydroxilated Ce(IV) ions from the oxidation of Ce(III) ions (Eq. (15), line 3 of the Pourbaix diagram). This process would raise the potential values, which could be related with the local growth of anodic areas observed in SVET maps after few hours of immersion of the rebar in the alkaline media. Thus, this reaction involves the dissolution of the conversion layer, and as observed from the SEM results, after one day of immersion in the alkaline solution, corroded areas were formed.

Table 1
Ratio Ce^{3+}/Ce^{4+} obtained from the XPS spectra

Species	Ce 0 h	Ce 20 h	Ce 6 days
Ce(IV)/Ce(III)	0.69	0.96	No detected

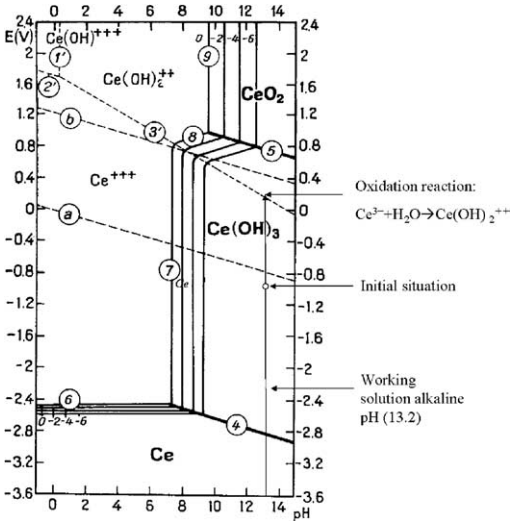

Fig. 14. Pourbaix diagram for cerium–water [35].

$$Ce^{3+} + H_2O \rightarrow Ce(OH)_2^{++} + 2H^+ + e^- \quad (15)$$

The corrosion potential remained cathodic for longer immersion times than the reference sample. This fact can be related with the delay observed in the zinc dissolution processes, and, thus in the formation of the protective layer of corrosion products.

SVET maps for the Ce-treated galvanized rebar showed that after few minutes of immersion in the alkaline solution, the cathodic activity was more generalized than the non-treated sample. This fact could be related with the cathodic reaction consuming the H^+ contained in the framework of Ce(III) oxide layer and also with the H^+ produced from oxidation of Ce^{3+} (Eq. (16)). This reaction should be promoting the low cathodic potentials measured for the Ce-treated sample during the first stages of contact with the alkaline media.

$$2H^+ + 2e^- \rightarrow H_2 \quad (16)$$

The results show that the cerium conversion layer, formed on the galvanized rebar surface delayed the dissolution of zinc when the rebar was immersed in the alkaline solution (pH 13.2) containing calcium ions. The Ce conversion layer was not able to hinder the hydrogen evolution that takes place during the passivation process due to the formation of calcium hydroxizincate ions on the rebar surface. Furthermore, Ce conversion layers did not seem to be stable in high pH solutions containing calcium ions.

4.2. La pre-treated rebars

When the galvanized rebar is immersed in the lanthanum nitrate solution anodic dissolution of zinc (Eq. (3)) and cathodic reduction of molecular oxygen takes place (Eqs. (4) and (5)) [34], like in the case of cerium treatment. Literature reports [34] that hydrated or hydroxylated La^{3+} reacts with the zinc hydroxide on the galvanized surface. These reactions lead to the formation of a lanthanum oxide and hydroxide protective layer over the galvanized surface (Eqs. (17) and (18)).

$$[Zn]OH + La^{3+}(OH_2) \rightarrow [Zn]OLa^{2+}(OH_2) + H^+ \quad (17)$$

$$[Zn]OH + La^{3+}(OH^-) \rightarrow [Zn]OLa^{2+}(OH^-) + H^+ \quad (18)$$

The La pre-treated rebar showed a barrier film composed by lanthanum hydroxides that could be identified by XPS in agreement with the Pourbaix diagram for lanthanum in water (Fig. 15) [35].

When the La-treated galvanized rebar is immersed in the alkaline solution, the La conversion film acts as a protective barrier between the galvanized surface and the alkaline

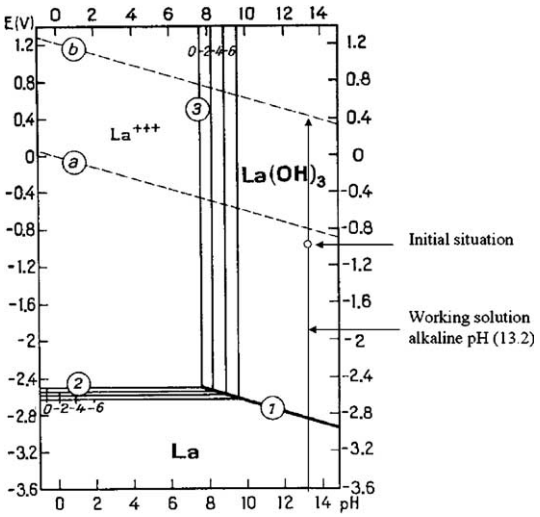

Fig. 15. Pourbaix diagram for lanthanum–water [35].

solution. Thus, the formation of zincate ions is delayed as well as the growth of calcium hydroxizincate crystals. This fact is in agreement with the SEM images obtained after one day of immersion in which no calcium hydroxizincate crystals could be observed. The reduction of anodic activity in SVET maps would indicate a more protective behaviour for the La-film.

The potential measurements for this sample should be related with the reactions consuming the H^+ contained in the framework of lanthanum oxides and hydroxides (Eq. (16)). SVET maps obtained after few minutes of immersion are in agreement with this fact, showing cathodic areas over the rebar surface. The cathodic potential values for this sample are maintained for more time than in the non-treated sample, which should be related with the delay in the formation of the CaHZn crystals that only takes place after dissolution of the conversion layer.

The results show that the La conversion layers formed over a galvanized rebar surface delayed the zinc dissolution when the rebar was immersed in a high alkaline medium with calcium ions. However, the La layers were not able to hinder the cathodic process of hydrogen evolution. The conversion film develops several cracks through which the corrosion products growth, covering the rebar surface.

In order to confirm the proposed mechanisms, further studies are needed to improve the stability of Ce and La conversion layers in high alkaline media and to help to understand how the conversion layer affects hydrogen evolution.

5. Conclusions

The conversion pre-treatments for galvanized reinforcing steel tested in this work reveal that conversion films based on cerium and lanthanum nitrate affected the corrosion processes of galvanized steel rebars during immersion in solutions of pH 13.2.

The mechanisms involved in the corrosion process seem to be slightly different for Ce and La conversion films. The presence of Ce conversion layer delays the formation of the corrosion layer that passivates the galvanized rebars in alkaline solutions containing calcium ions.

La conversion layer initially hindered Zn dissolution forming a barrier film over the galvanized surface. However, during immersion this layer flakes and dissolves allowing the reactions of Zn ions with the calcium ions.

For the conditions tested in this work, the cathodic reaction involving hydrogen evolution was not hindered by the presence of the cerium or lanthanum conversion films.

Acknowledgement

Collaboration CSIC (Spain)/GRICES (Portugal) 2004PT0004. M. Sánchez acknowledges a Fellowship from the Spanish Education Ministry (FPU program).

EFC is strongly acknowledged.

References

[1] Yeomans Stephen R, editor. Galvanized steel reinforcement in concrete. Elsevier; 2004.
[2] Andrade C, Macías A. In: Wilson AD, Nicholson JW, Prosser HJ, editors. Surface coating, vol. 2. Elsevier Applied Science; 1987. p. 137–89.
[3] Roetheli BE, Cox GL, Littreal WB. Met Alloys 1932;3:73–6.
[4] Macías A, Andrade C. Brit Corros J 1987;22:113–8.
[5] Fratesi R, Moriconi G, Coppola L. The influence of steel galvanization on rebars behaviour in concrete. In: Page CL, Bamforth PB, Figg JW, editors. Corrosion of reinforcement in concrete construction. UK: The Royal Society of Chemistry; 1996. p. 631.
[6] Sarmaitis RR, Rozovsky VG. In: 9th International Conference of Metallic Corrosion, Toronto, 1984. p. 390–5.
[7] Montemor MF, Simões AM, Ferreira MGS. Prog Org Coat 2001;43:274–81.
[8] Montemor MF, Simões AM, Ferreira MGS. Prog Org Coat 2002;44:111–20.
[9] Trabelsi W, Cecilio P, Ferreira MGS, Montemor MF. Prog Org Coat 2005;54:276–84.
[10] Ferreira MGS, Duarte RG, Montemor MF, Simões AMP. Electrochim Acta 2004;49:2927–35.
[11] Almeida E, Fedrizzi L, Diamantinio TC. Surface Coat Technol 1998;105:97–101.
[12] Aramaki K. Corros Sci 2001;43:2201–15.
[13] Aramaki K. Corros Sci 2002;44:1375–89.
[14] Aramaki K. Corros Sci 2002;44:1361–74.
[15] Aramaki K. Corros Sci 2002;44:1621–32.
[16] Kasten LS, Grant JT, Grebasch N, Voevodin N, Arnold FE, Donley MS. Surface Coat Technol 2001;140:11–5.
[17] García-Heras M, Morales AJ, Casal B, Galván JC, Radzki S, Villegas MA. J Alloys Comp 2004;380:219–24.
[18] Pepe A, Aparicio M, Ceré S, Durán A. J Non-Cryst Solids 2004;348:192.
[19] Aramaki K. Corrosion 1999;55:157.
[20] Hinton BRW, Wilson L. Corros Sci 1989;29:967–75.
[21] Hinton BRW. J Alloys Compd 1992;180:15–25.
[22] Aldykewicz AJ, Isaacs HS, Davenport AJ. J Electrochem Soc 1995;142:3342.
[23] Aballe A, Benthecourt M, Botana FJ, Marcus M. J Alloys Compd 2001;323–324:855–8.
[24] Rudd AL, Breslid C, Mansfeld F. Corros Sci 2000;42:275–88.
[25] Bernal S, Botana FJ, Calvino JJ, Marcos M, Pérez-Omil J, Vidal H. J Alloys Comp 1995;225:638–41.

[26] Alonso C, Acha M, Andrade C. Admixtures for concrete improvement of properties. UK: Chapman and Hall; 1990. p. 219–28. Edt Vazquez.
[27] Stern M, Geary AL. J Electrochem Soc 1957;1:56–63.
[28] Macías A, Andrade C. Brit Corros J 1987;22:162–71.
[29] Blanco MT, Andrade C, Macías A. Brit Corros J 1984;19:41–8.
[30] Bird CE. Corros Prevent Contr 1964;7:17–21.
[31] Lieber W, Gebauer J. Zement-kalk-Gips 1969;4:161–4.
[32] Liebau F, Amel-Zadeh A. Kist Tech 1972;7:221–7.
[33] Arenas MA, de Damborenea JJ. Surface Coat Technol 2004;187:320.
[34] Aramaki K. Corros Sci 2001;43:1573–88.
[35] M. Pourbaix, Atlas of electrochemical equilibria in aqueous solutions. NACE, Centre Belge d'Etude de la Corrosion (CEBELCOR), USA, 1974.